



Simulation of screw runner for cylindrical basin of gravitational water vortex power plant (GWVPP)

Niroj Bhattarai ^{a,*}, Raj Kumar Chaulagain ^a

^a Department of Automobile and Mechanical Engineering, Thapathali Campus, IOE, Tribhuvan University, Nepal

ARTICLE INFO

Article history:

Received 19 Aug 2022
Received in revised form
15 Sep 2022
Accepted 18 Nov 2022

Keywords:

Gravitational Water Vortex Power Plant (GWVPP)
Screw Type Runner
Vertical Archimedes Screw Runner
Two-Phase Modeling

Abstract

Gravitational water vortex plant is an emerging technology to extract energy created from vortex formation in ultra-low head range. This research was conducted to test a modification in Archimedes screw as a new type of runner for Gravitational water vortex plant, considering atmospheric opening at the topmost surface of the channel. After CFD optimization, the optimum dimension for screw runner was found to have 2 blades, 267 mm height, 180 mm radius from center axis, 160 mm pitch and is positioned 235.5 mm from the top surface of the gravitational water vortex basin. Runners with blade number two and three were found to be more efficient than single and four blade runners. Out of all runners, the efficiency and output power of the two-blade screw runner was found to be a maximum of 4.07 % and 1.004 Watts respectively at 55 rpm. Further analysis of the optimized runner was done by varying the inlet speed of the water at the canal from 0.25 m/s to 0.75 m/s and found that efficiency increased with increasing inlet speed.

©JIEE Thapathali Campus, IOE, TU. All rights reserved

1. Introduction

The hydropower sector has become the most demanded energy source because of its cleaner generation. Low head power plants are most suitable for areas that are not connected to the grid or areas of difficult terrain. Using a low hydraulic head of up to 2 meters, the gravitational water vortex power plant is a kind of micro hydro vortex turbine system that can generate rotational energy from a flowing fluid. Figure 1 shows the application range of hydraulic turbines. Because there is just one moving element in this kind of micro hydro, it operates more simply and requires less maintenance, increasing its operational life. Screw turbines consist of the cylindrical shaft along with helical surfaces (flights) thus forming a screw shaped structure. The water enters from the top of the screw along the flights that rotate the shaft which then rotates the rotor of the generator. In a developing nation like Nepal, rural areas due to a lack of infrastructure are not connected to the national grid. Such rural areas with some canal flow can benefit from low-head hydro installations. Vortex-based plants

operate on natural water flow and do not require a large storage reservoir during the construction phase. Also, some small portion of water from a river can be directed into a canal and can be used for operation.

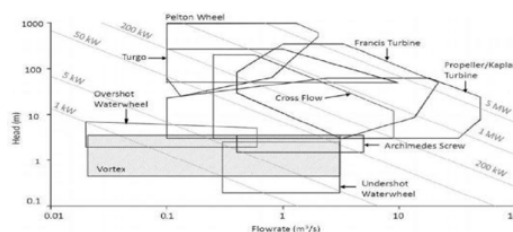


Figure 1: Application range of hydraulic turbines [1]

For a sustainable future, water energy, which is a clean, affordable, and environmentally friendly form of power generation, is crucial. Large-scale electricity production may lead to environmental pollution and climate change effects. On the other hand, they are very costly. The terai and hill region in Nepal has water resources with very low head and medium to high discharge conditions.

*Corresponding author:

bhattarainiroj414@gmail.com (N.B.)

The goal of this work is to further the understanding of ultra-low head gravitational water vortex turbines that are suitable for producing electricity in such areas. This form of turbine may be put in rural, isolated areas with some sort of canal system flow.

Being a new kind of technology, research in the field of GWVPP is less as compared with other types of hydro plants. Past studies mainly focused on studying the parameters of runners and their optimization for achieving optimum efficiency [2]. Various studies focused on numerical and experimental methods for optimizing the turbine, as it is the most crucial part of the power plant. They mainly focused on blade numbers, position placement in the basin, blade angle, and size of blades. Many researchers have assumed a closed system of canals whereas in actuality canals are open to the atmosphere.

M. Rahman et al [2] went through past research to search gap in vortex technology and developed recommendations for the improvement of GWVPP. They also observed that maximum efficiency obtained in research was approximately 30% while the installation companies claimed about 50% efficiency with 500W to 20kW of power generation. They indicated that there are several opportunities to increase GWVPP runner efficiency. Before optimizing the form and profile of the blades, a suitable turbine should be chosen to achieve optimal efficiency. Bajracharya and Chaulagain [3] conducted an experimental study to develop a novel low head water turbine for free flowing streams suitable for micro-hydropower in Nepal's Terai area. According to the study's findings, a cylindrical basin's height, diameter, and bottom exit hole are set under a fixed discharge situation. The study also implies that the exit hole is smaller than the vortex minimum diameter, which is at the lowest level. Dhakal et al [4] studied and found that curved blade profile had more efficiency than straight bladed profile. According to their study, curved blade profile had a greater maximum efficiency of 82.4 percent compared to 46.31 percent of straight blade and the twisted blade profile's 63.54 percent. They also suggested in their study that vortex generation near the orifice weakened gradually because of the cylindrical shape thus conical shaped basins were found to be more efficient. Additionally, they concluded that the turbine extracts maximum efficiency of 36.84 percent when the basin is between 65 and 75 percent of its overall height. In a parametric experimental analysis of the GVPP operating conditions, Power et al. [5] investigated the effects of the intake conditions, flow rates, blade diameters, and blade numbers on the turbine speed, torque, and vortex height. The study demonstrated that when blade size and number increase, turbine efficiency also improves.

An experimental analysis conducted for maximizing output for low flow rates and head identified a screw turbine with a screw angle from 20 to 25 degrees and flow rates below 1.5 liters per second to have an efficiency of around 90% where RPM is kept constant for reducing overflow losses [6].

Computational study on the performance of helical blade profile turbine in gravitational water vortex plant showed the trend of increment and decrement of turbine efficiency with an increase of submergence of the turbine in the basin. Also from both computational and experimental results, they showed that the use of helical turbines and their fabrication would be complex and costly for they produce very less power. The turbine model studied in the research was found to have a maximum efficiency of less than 1 % [7]. In a study by Bouvant et al [8], the performance of the Archimedes screw was evaluated for maximizing power coefficient and found under optimal design conditions that the angle of the blade concerning the center axis was 73.94 degrees, the pitch was 220 mm and hub diameter ratio with blade outer diameter was 0.1. A study of the performance of screw-type runners in gravitational vortex [9] found that optimum pitch for screw runner was 100 mm for curved profile of single blade of 318 mm height and which for the reference basin taken gave maximum efficiency of 7.03 % at 100 rpm. Regmi et al [10] performed multiphase CFD analysis with open top surface where exit hole and taper of GWVPP basin were varied and corresponding variations in flow effect were studied. Finally, a runner was designed for the reference basin and developed using bronze metal and their computational and experimental results were compared. Computational analysis showed 7.93% efficiency while the experimental maximum efficiency was found 52.58 % greater than computational.

New types of turbine models have to be designed and tested in vortex flow which could turn out to be more efficient than the previously designed runners. Thus, with the aim of exploring a new turbine design in vortex setup and studying its behavior with considerations of efficiency factor, this study considers a modification of Archimedes screw turbine design. Schematic of Archimedes screw is shown in figure 2. This study solely focuses on the development of a new type of runner for two-phase modeling of air and water in gravitational vortex plant considering open atmospheric conditions at inlet channel top surface.

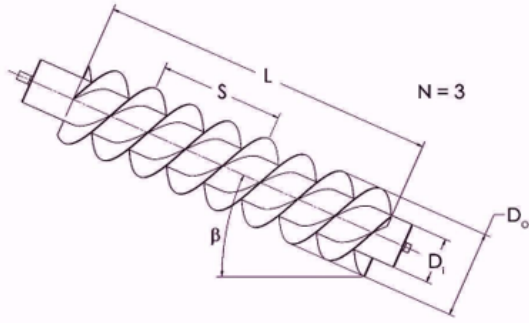


Figure 2: Schematic diagram of Archimedes screw [11]

2. Design Methodology

2.1. Cylindrical basin type GWVPP canal

The dimensions of the gravitational water vortex power plant with a cylindrical basin are taken from a past research paper by [9] as shown in figure 3. Similar geometry of basin was taken for cylindrical type vortex basin in this study. CAD modeling of the basin and runner was done in 2017 Solidworks software.

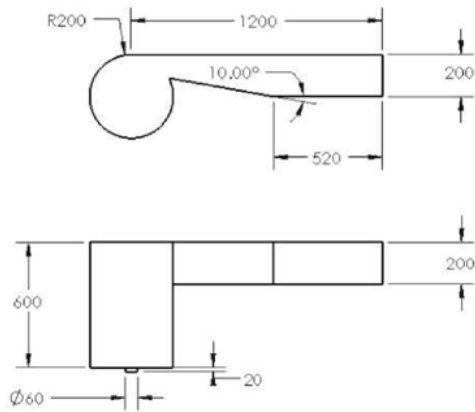


Figure 3: 2D of basin structure

2.2. Cylindrical screw type runner

Based on Archimedes' screw design [12], a cylindrical screw type runner is designed. Archimedes screw being the central component, its important design parameters are tabulated in table 1 with pictorial representation in figure 4.

For, vertical axis screw design angle of inclination of screw β was taken 90° . Blade outer diameter was selected as 360 mm on basis of the dimension of the cylindrical basin to keep 20 mm clearance. Fill height, and upper and lower level-like parameters had no relevance to the 90° inclination of the submerged turbine. In the

Table 1: Parameters of Archimedes screw

D_i	Inside diameter
D_o	Outside diameter
L	Total length
β	Angle of inclination
N	Number of helical planed surfaces
S	Screw pitch
f	Fill height
h_u	Upper level
h_L	Lower level

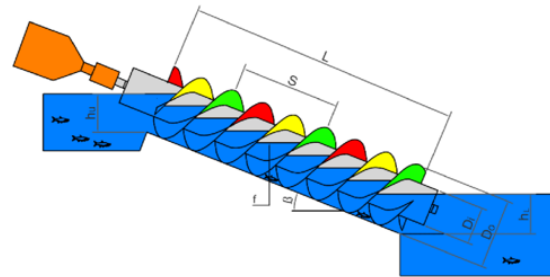


Figure 4: Archimedes screw parameters [12]

past research by [8], they suggested for the optimum power coefficient angle of inclination of blade concerning axis was taken as 73.94° , and pitch for initial design was taken 220 mm. Therefore, the value of pitch and inclination of the blade was taken the same as in the previous research. Initially blade length was taken as one pitch and due to the inclination angle height of the runner was slightly more than the pitch. Past research by Bouvant et al [8] suggested that the inner diameter be 0.1 times that of the outer diameter which came to be 36 mm. Also in another research work [9] in a conical basin set up, they had taken 40 mm for the shaft. So, 40 mm inner shaft diameter was considered in this research.



Figure 5: Proposed Screw turbine model

It can be considered as a modified Archimedean screw turbine where several blade profiles are one and some other geometrical parameters are referenced from various past studies [8], [9]. The proposed model of the screw turbine is similar to the figure 5. Initial dimension of the assumed screw is shown as in figure 6.

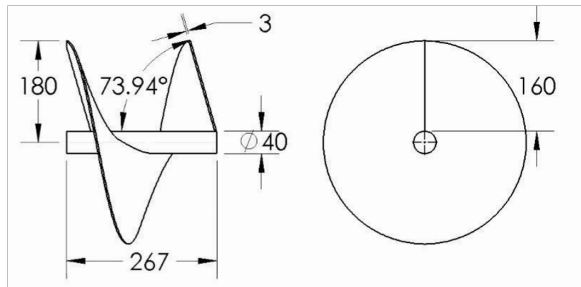


Figure 6: Runner (Dimension of initial assumption)

2.3. Numerical model development

All numerical simulation was performed in ANSYS software to calculate discharge flow rates and torques developed by the runner for a given angular velocity. Power input and power produced by the runner can be determined from the calculated discharge and torque thus the efficiency of the screw runner can be calculated [13]. ANSYS 2021 R1 version of the software was used in numerical simulations and SOLIDWORKS 2017 as CAD modeling software. Models drawn in SOLIDWORKS were imported to ANSYS in ACIS format. The advanced meshing of the ANSYS workbench was used for meshing. Mesh metrics orthogonal quality, skewness etc. were monitored to obtain better mesh without affecting the accuracy of the solution. Model-

ing was done as a stationary domain for the basin canal and a rotary domain for the runner part [13]. Named selections for various parts were done so that mesh size can be altered and refined for those parts.

2.4. Physics setup

Multiphase Eulerian fluid approach was used as fluids air, water are used for phase modeling. Reference pressure and temperature of the domain were set at 1 atm and 25° C respectively. Buoyancy reference density was taken as the same as air density (1.2 kg/m³). Fluid properties of air and water were taken by default of ANSYS software. In generating vortex flow gravity has essential role, so buoyant conditions were defined in the simulation. The model used for turbulence in this study is SST $k-\omega$. The SST $k-\omega$ model gives more precise values of torque [14] and it also provides robustness while reducing the computational time of the run as compared with other turbulence models such as Reynolds Stress Model [15]. A high-resolution advection scheme and High-resolution turbulence numeric were used for solver preference in setup. Total of 2000 iterations and 0.0001 residual target was taken [10], [14]. Physics set up including boundary conditions are shown in figure 7.

2.5. Mesh Independence test

A Mesh independence study is done initially for starting CFD simulations to ensure that solutions obtained are not dependent on mesh resolutions and also to reduce computational effort for similar results. Five different element sizes mesh were taken ranging from 312112 to 731803 tetrahedrons. The torque acting on the runner along the y-axis was observed for all cases and number

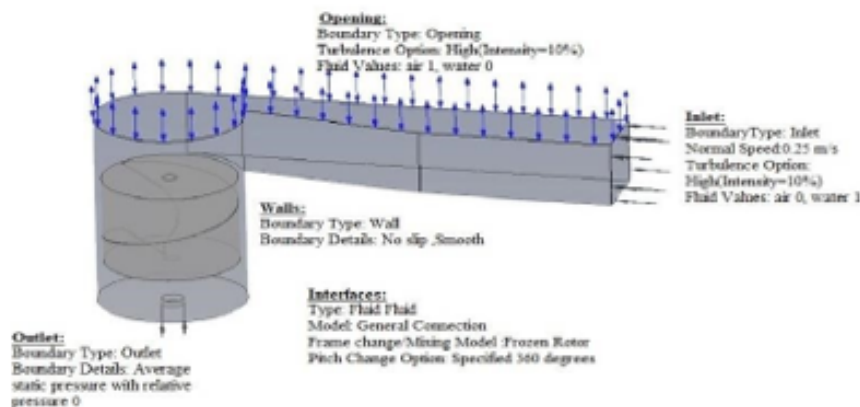


Figure 7: Physics setup for initial screw type runner

of mesh elements vs. torque graph was drawn.

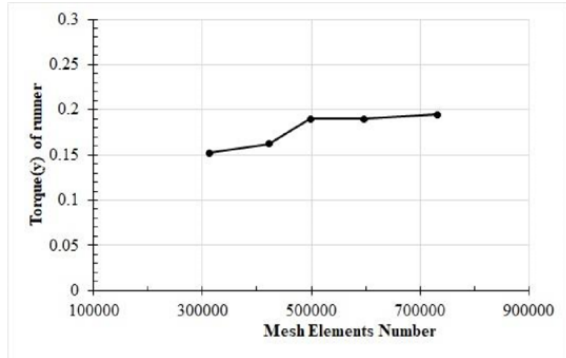


Figure 8: Mesh independence test result

From figure 8, it can be shown that after increasing mesh elements from 498919 there is no rapid rise in torque. The torque acting on the runner at 731803 elements differs from torque acting when mesh size was 498919 by only 2.5% which is less than 3%. Also, the time for completion of simulation for 498919 elements was 7.5 hours as compared to 10 hours for 731803. So for other simulation runs to tradeoff between accuracy and time took for simulation 500000 number of elements was used.

3. Result and Discussion

3.1. Optimizing the initial runner by varying parameters

Different CAD models were simulated for steady state condition at 40 rpm in order to optimize the previously assumed single blade screw runner. Due to opening type boundary on the top surface discharge flow rate differs between outlet and inlet, hence discharge flow rate at the outlet was determined by using the ANSYS code. Torque developed at the runner was also determined by ANSYS code for each simulation. Power input, power output, and efficiency were then calculated using equations given below.

$$\text{Input Power} = \rho \times g \times Q \times H \quad (1)$$

Where,

$$\begin{aligned} \rho &= \text{water density} = 998 \text{ kg/m}^3 \\ g &= \text{gravitational acceleration} = 9.81 \text{ m/s}^2 \\ H &= \text{Head up to runner mean height} \end{aligned}$$

Discharge Flow rate,

$$Q = \frac{\text{mass flow @ Outlet}}{998} \quad (2)$$

$$\text{Power developed at runner} = T \times \omega \quad (3)$$

Where,

$$\begin{aligned} \text{Angular velocity } (\omega) &= \frac{2}{60} \text{ d/sec} \\ \text{Torque (T)} &= \text{torque @ runner} \\ &\text{default Nm} \end{aligned}$$

Finally,

$$\text{Efficiency } (\eta) = \frac{\text{Power developed at runner}}{\text{Input Power}} \times 100\% \quad (4)$$

For optimizing the initially proposed runner, various parameters like pitch, the height of runner, blade radius, the position of runner, and revolutions were analyzed varying one parameter at a time while keeping others constant. Torque, discharge, power, and efficiency obtained were analyzed and the most efficient configuration among all was chosen for further simulations. The efficient height of the runner was chosen after finalizing the pitch parameter that gives maximum efficiency and so on continued for blade radius, position, and rpm till all the considered parameters were optimized.

3.1.1. Effect of pitch lengths

The pitch of the initially assumed single blade screw was varied from 100 mm to 220 mm for steady-state simulations of 40 rpm maintaining other aspects like length, and position from top surface constant. The values of torque, flow rate, input and output powers developed by the runner, and efficiency were calculated. The graphs of power and efficiencies are shown in figure 9 depict that a screw runner having a pitch of 160 mm with all other parameters constant had generated maximum output power of 0.826 watts with discharge flow 0.006987 m^3/s and efficiency 3.61%. Thus, the pitch length of 160mm, which gave maximum efficiency for all other similar parameters was selected.

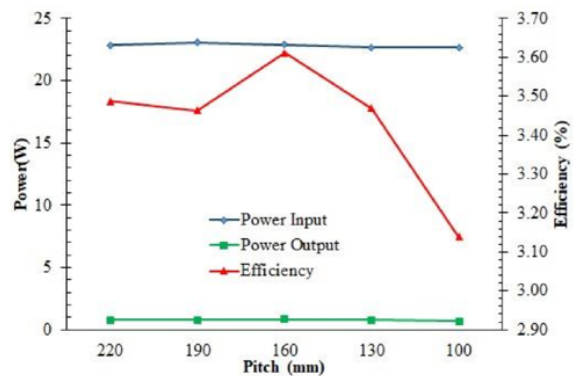


Figure 9: Variation of power and efficiency of single blade screw with a pitch

3.1.2. Effect of heights of the runner

The height of runner domain was varied between 236 mm to 368 mm with increments of 33 mm maintaining a constant pitch of 160mm from the previous result and other parameters for analysis at steady state of 40 revolution per minute and runner mean height from the top at 400 mm. The values of torque, flow rate, input and output powers developed by the runner, and efficiency are calculated from the simulations. The graphs of power and efficiencies shown in figure 10 depict that a single blade screw runner having a height of 269 mm and 160 mm pitch with all other parameters constant had generated maximum output power of 0.922 watts with discharge flow rate $0.006869 \text{ m}^3/\text{s}$ and efficiency 3.43%. Thus, the runner height of 269mm, which gave maximum efficiency for all other similar parameters was selected.

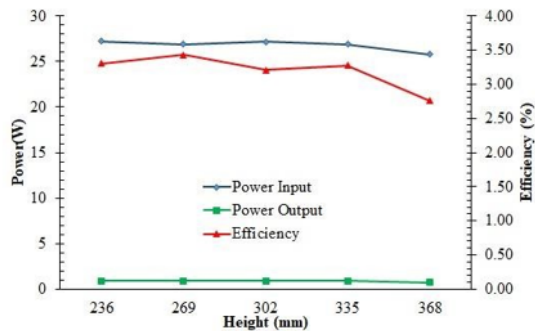


Figure 10: Variation of power and efficiency of single blade screw with height

3.1.3. Effect of runner radius

Blade radius of single blade runner domain was varied between 150 mm to 190 mm with increments of 10 mm maintaining a constant pitch of 160mm and constant runner domain height of 269 mm from the previous result for runner analysis at a steady speed of 40 rpm and runner mean height from the top at 400 mm. The values of torque, flow rate, input and output powers developed by the runner, and efficiency are calculated from the simulations. The graphs of power and efficiencies are shown in figure 11 depict that the screw runner having a blade radius of 180 mm with all other parameters constant had generated maximum output power of 0.922 watts with discharge flow $0.006869 \text{ m}^3/\text{s}$ and efficiency 3.43%. Thus, the runner radius of 180 mm, which gave maximum efficiency for all other similar parameters was selected.

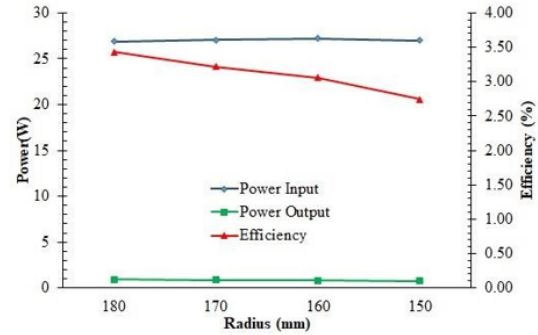


Figure 11: Variation of power and efficiency of single blade screw with radius

3.1.4. Effect of runner positions (Blade no 1)

Positions of the single blade runner domain with respect to top surface was varied from 205.5 mm to 325.5 mm with increments of 30 mm maintaining a constant pitch of 160mm, constant blade radius of 180 mm, and constant runner domain height of 269 mm from the previous result for CFD analysis of runner at steady state of 40 rpm. Further, additional positions 180.5 mm and 220.5 mm from the top positions were simulated deviating both sides 20 mm from the 205.5 mm position. The values of torque, flow rate, input and output powers developed by the runner, and efficiency are calculated. The graphs of power and efficiencies are shown in figure 12 depict that the screw runner positioned 205.5 mm from the top surface having the mean head of 0.355 mm with all other parameters constant had generated output power of 0.8762 watts with discharge flow of $0.0069137 \text{ m}^3/\text{s}$ and maximum efficiency 3.81%. Thus, runner position for the head of 0.340 mm, which gave maximum efficiency for all other similar parameters was selected.

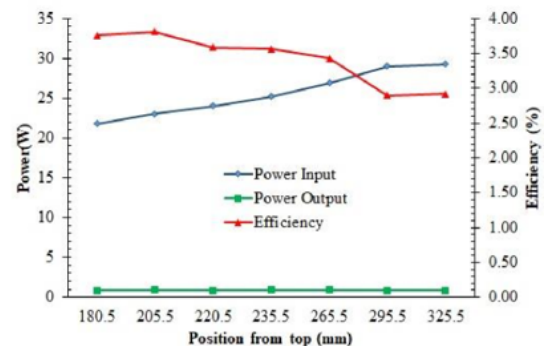


Figure 12: Variation of power and efficiency of single blade screw with radius

Combining all of the above maximum efficiency obtaining height, pitch, blade radius, and position of a runner on the basin, dimensions for optimized single blade runner are taken as in table 2.

Table 2: Parameters for optimized single blade screw runner

S.N.	Parameters	Value (mm)
1	Number of blades	1
2	Radius of Runner	180
3	Blade Thickness	3
4	Height of runner	267
5	Pitch of screw runner	160
6	Shaft Diameter	40
7	The angle of inclination of the blade	73.94 degrees
8	Runner Position from the top surface	205.5

3.1.5. Effect of runner positions (Blade No 2)

Positions of the two-blade runner domain with respect to top surface varied from 205.5 mm to 265.5 mm with increments of 30 mm maintaining a constant pitch of 160mm, constant blade radius of 180 mm, and constant runner domain height of 269 mm from the previous result for CFD analysis of single blade runner at steady state of 40 rpm. The values of torque, flow rate, input and output powers developed by the runner, and efficiency are calculated. The graphs of power and efficiency shown in figure 13 depict that two blade screw runners positioned 235.5 mm from the top surface having the mean head of 0.370 mm with all other parameters constant had generated output power of 0.9408 watts with discharge flow of $0.0069194 \text{ m}^3/\text{s}$ and maximum efficiency of 3.75%. Thus, runner position for the head of 0.370 mm, which gave maximum efficiency for all other similar parameters was selected.

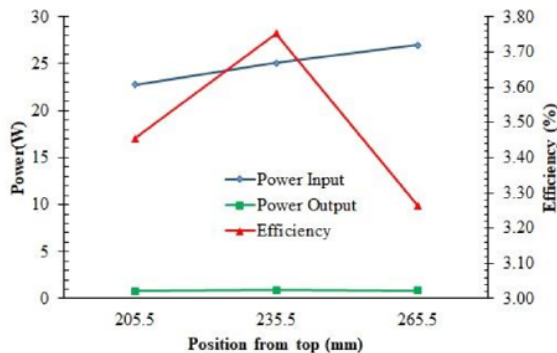


Figure 13: Variation of power and efficiency of two blade screw with position

3.1.6. Effect of runner positions (Blade No 3)

Similarly, positions of three-blade screw domain with respect to top surface was varied from 205.5 mm to 265.5 mm with increments of 30 mm. The graphs of power and efficiency shown in figure 14 depict that three blade screw runners positioned 205.5 mm from the top surface having the mean head of 0.340 mm with all other parameters constant had generated output power of 0.869 watts with discharge flow of $0.0069345 \text{ m}^3/\text{s}$ and maximum efficiency 3.77%. Thus, runner position for the head of 0.340 mm, which gave maximum efficiency for all other similar parameters was selected.

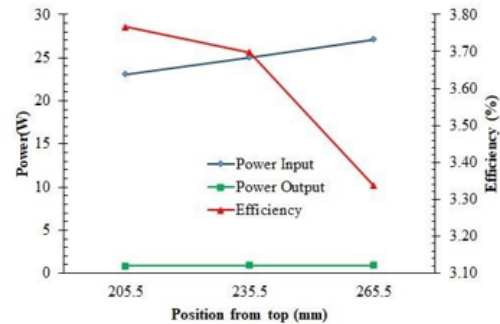


Figure 14: Variation of power and efficiency of three blade screw with position

3.1.7. Effect of runner positions (Blade No 4)

Positions of four-blade screw with respect to top surface was varied from 205.5 mm to 265.5 mm with increments of 30 mm. The graphs of power and efficiency

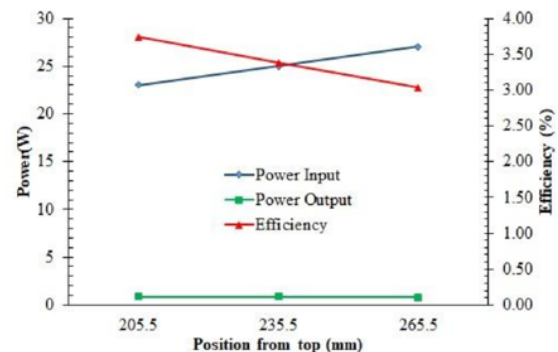


Figure 15: Variation of power and efficiency of three blade screw with position

are shown in figure 15 depict that the four-blade screw runner positioned 205.5 mm from the top surface having the mean head of 0.340 mm with all other parameters constant had generated output power of 0.8616 watts

with a discharge flow rate $0.0069207 \text{ m}^3/\text{s}$ and maximum efficiency 3.74%. As a result, the 0.340 mm runner position for the head was chosen since it provided the most efficiency.

3.2. Performance Analysis

3.2.1. Optimized single blade screw runner

Steady-state CFD analysis by the varying rotation speed of the optimized screw runner of dimensions as mentioned in table 2 was performed. From figure 16 it infers that at rpm of 40, single blade screw runner developed maximum power of 0.876 Watts, discharge of $0.0069137 \text{ m}^3/\text{s}$, and maximum efficiency of 3.807%.

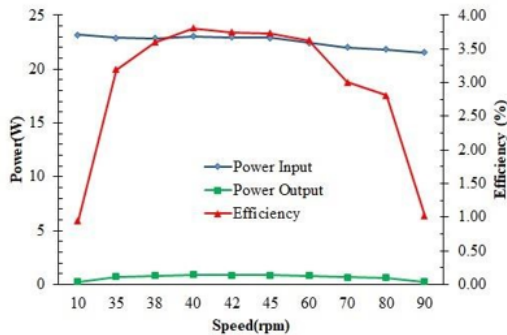


Figure 16: Variation of power and efficiency of single blade screw with speed

3.2.2. Optimized two-blade screw runner

Steady-state CFD analysis by the varying rotation speed of the position-optimized two-blade screw runner was performed. The results obtained as shown in figure 17 infer that at rpm of 55, two blade screw runner developed peak power of 1.004 Watts, discharge $0.0068144 \text{ m}^3/\text{s}$, and maximum efficiency 4.068%.

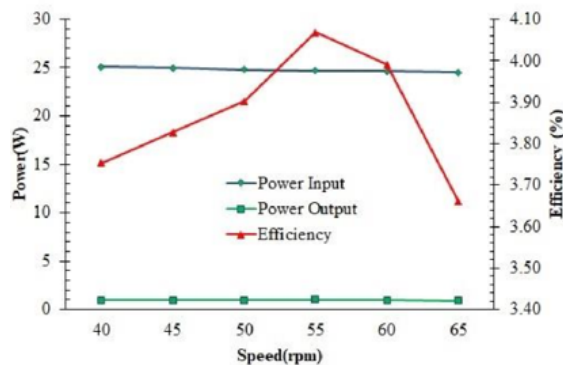


Figure 17: Variation of power and efficiency of the two-blade screw with speed

3.2.3. Optimized three-blade screw runner

Similarly, steady state CFD analysis by the varying rotation speed of the position optimized three blade screw runner was performed. Results found as in figure 18 showed that at rpm of 45, three blade screw runner developed maximum power of 0.939 Watts, discharge of $0.006947 \text{ m}^3/\text{s}$, and maximum efficiency of 4.063%.

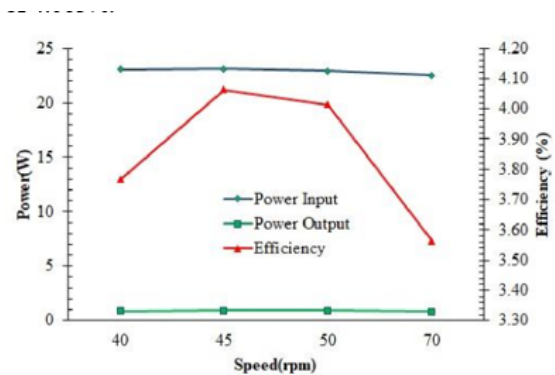


Figure 18: Variation of power and efficiency of the three-blade screw with speed

3.2.4. Optimized four-blade screw runner

Steady-state CFD analysis by the varying rotation speed of the position optimized four-blade screw runner was performed as shown in figure 19. It was found that at an rpm of 55, a four-blade screw runner developed maximum power of 0.8822 Watts, discharge of $0.0068022 \text{ m}^3/\text{s}$, and maximum efficiency of 3.896%.

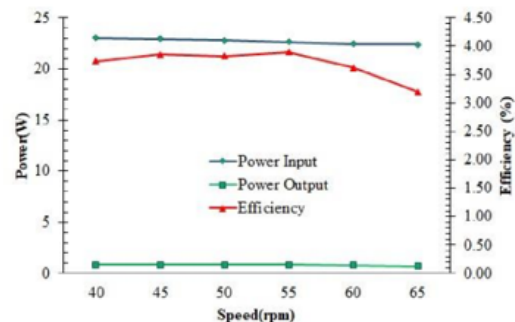


Figure 19: Variation of power and efficiency of the four-blade screw with speed

Among the different number of blades runners, a runner with two blades was found to have a maximum efficiency of 4.07% at 55 rpm. The dimension of the optimized screw two-blade runner is shown in figure 16.

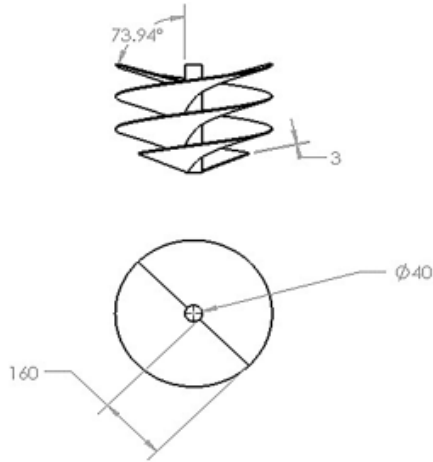


Figure 20: Optimized two-blade runner

The simulations of the two blade runner are shown in below figures 20 and 21 .

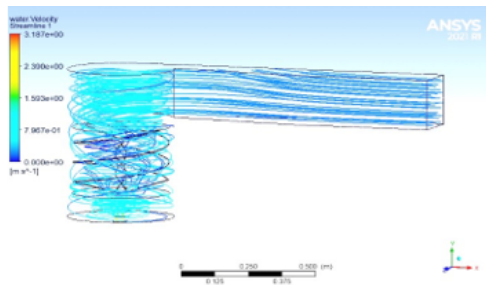


Figure 21: Water velocity streamline of optimized (two blade) runner

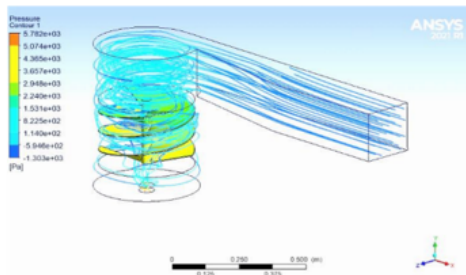


Figure 22: Pressure contour of optimized (two blade) runner

3.2.5. Mesh independence of optimized runner (2 blades)

Analysis of screw type single and multi-blade runners was done with 500000 mesh elements with a mesh size of 12 mm. Independence test for the final optimized

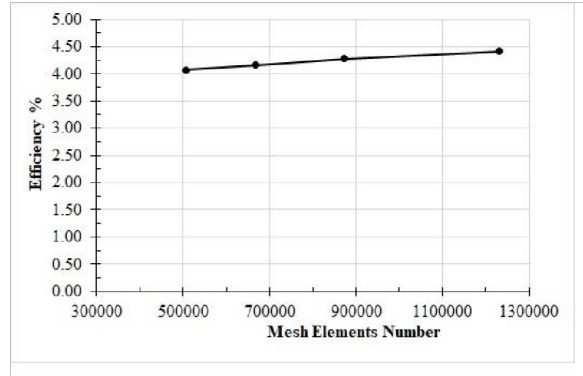


Figure 23: Mesh independence of optimized runner

runner was done by taking efficiency as a parameter. Mesh elements numbers were changed from 506999 to 1230093 as shown in figure 22. The efficiency of the runner changed according to mesh size. Efficiency varied from 4.07% at 506999 to 4.42% at 123009 number of elements. As mesh number increased by 140% elements, a difference of 8.65% was found in efficiency which is below 10%. Thus simulations above produced findings that were fairly accurate when mesh elements of five lakhs was used.

3.2.6. Inlet speed variation

Inlet speed was varied from 0.25m/s to 0.75 m/s at an interval of 0.25 for the simulation of a twoblade screw runner at a constant rpm of 55 rpm to study its effect on the performance of the runner. Other setup conditions were taken similarly in all cases and only the inlet flow speed of the water was altered. As shown in figure 23, the power and efficiency of two blade screw runner increased with the inlet flow speed of water in the canal.

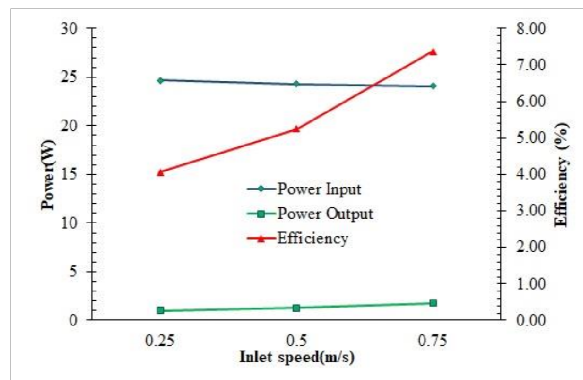


Figure 24: Variation of power and efficiency of the two-blade screw with inlet speed

4. Conclusion

Past studies related to gravitational vortex turbine development are studied in this research. Modified Archimedes screw turbine for reference cylindrical basin is developed utilizing CFD analysis. Various parameters are considered for optimizing the screw runner. Dimension of optimum screw runner was determined to have two no of blades, 267 mm height, 180 mm radius from the center axis, 160 mm pitch and is positioned 235.5 mm from the top surface of the gravitational water vortex basin. The CFD analysis was performed for all single and multi-blade profiles of the runner at different rpm speeds. Maximum efficiency of single, two, three and four blade runners were found as 3.8%, 4.07%, 4.06%, 3.9% respectively at 40, 55, 45 and 55 rpm. Among all, two blade design was found to have a maximum output power of 1.004 Watts and maximum efficiency of 4.07% at 55 rpm. For similar other setups, the inlet water speed of the canal was increased slightly and found that efficiency increased up to 7.37% for flow at 0.75 m/s speed.

CFD analysis can be done with fine quality mesh consideration. This model of runner can also be further studied in the conical basin setup and efficiency can be compared and studied. Further modifications can be done to the blade profile by using curved blades and varying angles of attachment at the same time. An experimental setup can be done to validate the theoretical analysis result. Moreover, modifications can be done in the runner during the experiment to check for efficiency improvisation and an improved model can be rerun in CFD simulations by varying setup and boundary conditions. Varying of setup conditions in ANSYS and matching the results to experimental case could be a milestone to other researchers who wish to perform vortex simulation in gravitational vortex power plant.

Acknowledgement

No financial aid were received for the completion of this project. The authors would like to thank all supportive faculty members of IOE Thapathali campus for their help and guidance regarding the subject matter.

References

- [1] Timilsina A B, Mulligan S, Bajracharya T R. Water vortex hydropower technology: a state-of-the-art review of developmental trends[J/OL]. *Clean Technologies and Environmental Policy*, 2018, 20(8): 1737-1760. DOI: [10.1007/s10098-018-1589-0](https://doi.org/10.1007/s10098-018-1589-0).
- [2] Rahman M, Tan J, Fadzilita M, et al. A review on the development of gravitational water vortex power plant as alternative renewable energy resources[C/OL]// IOP Conference Series: Materials Science and Engineering: volume 217. IOP Publishing, 2017: 012007. DOI: [10.1088/1757899X/217/1/012007](https://doi.org/10.1088/1757899X/217/1/012007).
- [3] Bajracharya T R, Chaulagai R. Developing innovative low head water turbine for free-flowing streams suitable for micro-hydropower in flat (terai) regions in nepal[J]. Kathmandu: Center for Applied Research and Development (CARD), Institute of Engineering, Tribhuvan University, Nepal, 2012.
- [4] Dhakal S, Timilsina A B, Dhakal R, et al. Comparison of cylindrical and conical basins with optimum position of runner: Gravitational water vortex power plant[J/OL]. *Renewable and Sustainable Energy Reviews*, 2015, 48: 662-669. DOI: [10.1016/j.rser.2015.04.030](https://doi.org/10.1016/j.rser.2015.04.030).
- [5] Power C, McNabola A, Coughlan P. A parametric experimental investigation of the operating conditions of gravitational vortex hydropower (gvhp)[J/OL]. *Journal of Clean Energy Technologies*, 2016, 4(2): 112-119. DOI: [10.7763/jocet.2016.v4.263](https://doi.org/10.7763/jocet.2016.v4.263).
- [6] Kashyap K, Thakur R, Kumar S, et al. Identification of archimedes screw turbine for efficient conversion of traditional water mills (gharats) into micro hydro-power stations in western himalayan regions of india: An experimental analysis[J/OL]. *International journal of renewable energy research*, 2020, 10 (3). DOI: <https://doi.org/10.20508/ijrer.v10i3.11176.g8020>.
- [7] Joshi S, Jha A K. Computational and experimental study of the effect of solidity and aspect ratio of a helical turbine for energy generation in a model gravitational water vortex power plant[J/OL]. *Journal of Advanced College of Engineering and Management*, 2021, 6: 213-219. DOI: [10.3126/jacem.v6i0.38360](https://doi.org/10.3126/jacem.v6i0.38360).
- [8] Bouvant M, Betancour J, Velásquez L, et al. Design optimization of an archimedes screw turbine for hydrokinetic applications using the response surface methodology[J/OL]. *Renewable Energy*, 2021, 172: 941-954. DOI: <https://doi.org/10.1016/j.renene.2021.03.076>.
- [9] Maharjan A, Chaulagain R K. Development of screw type runner for conical basin of gravitational water vortex power plant[J/OL]. 2021. <https://www.researchgate.net/publication/359158929>.
- [10] Regmi N, Dura H, Shakya S R. Design and analysis of gravitational water vortex basin and runner[C]// *Proceedings of IOE Graduate Conference: volume 7*. 2019: 157-164.
- [11] Kozyn A. Power loss model for archimedes screw turbines[D/OL]. University of Guelph, 2016. <http://hdl.handle.net/10214/9617>.
- [12] YoosefDoost A, Lubitz W D. Archimedes screw turbines: A sustainable development solution for green and renewable energy generation—a review of potential and design procedures[J/OL]. *Sustainability*, 2020, 12(18): 7352. DOI: <https://doi.org/10.3390/su12187352>.
- [13] Gautam A, Sapkota A, Neupane S, et al. Study on effect of adding booster runner in conical basin: gravitational water vortex power plant: a numerical and experimental approach[C/OL]// *Proceedings of IOE graduate conference*. 2016: 107-113. <http://conference.ioe.edu.np/ioegc2016/papers/IOEGC-2016-14.pdf>.
- [14] Khan N H. Blade optimization of gravitational water vortex turbine[J/OL]. PhD diss., Tesis MT, Teknik Mesin, Ghulam Ishaq Khan Institute of Engineering Sciences and Technology, 2016. <https://www.academia.edu/34334744>.
- [15] Bajracharya T R, Shakya S R, Timilsina A B, et al. Effects of geometrical parameters in gravitational water vortex turbines with conical basin[J/OL]. *Journal of Renewable Energy*, 2020. DOI: <https://doi.org/10.1155/2020/5373784>.